Optical and Quantum Electronics (2024) 56:617
https://doi.org/10.1007/s11082-024-06299-6

# Synthesis, morphology, vibrational, and physical characterization of DGEBA epoxy doped liquid crystal organic polymeric systems (EDLCPSs) for high-performance embedded capacitors

**W. Jilani[1,2] · A. Bouzidi[2] · Slim Elleuch[3] · H. Guermazi[2]**

Received: 13 November 2023 / Accepted: 4 January 2024 / Published online: 1 February 2024


**Abstract**
The synthesis, morphology, and physical characterization of neat epoxy and DGEBA epoxy doped liquid crystal organic polymeric systems (EDLCPSs) have been investigated. Morphological properties of both systems were examined by SEM techniques. The small size of the LC droplets (0.224 µm) is also consistent with the presence of nitrile groups. The Fourier transform infrared (FTIR) and Raman spectra of the EDLCPSs detect a vibration band at 2229 $cm^{-1}$ is attributed to C≡N stretching vibrational band. The optical band gap and refractive index have been studied using UV–visible spectroscopy. The calculated optical band gap of the EDLCP system shows a red shift as compared to neat epoxy. Our optical parameters were found to increase in the EDLCPSs. In the UV region, the systems block UV light up to a wavelength of about 380 nm which is an efficiency of UV light shielding devices. The photoluminescence (PL) is measured as a function of temperature for both systems. The integrated PL intensity decreases below 300 °C for the neat epoxy and lower than 220 °C for the EDLCPSs when increasing temperature is an effect related to the phonon diffusion (i.e., the photo-created pairs electron–hole). After 320°C, the neat epoxy system shows a completely inverted behavior when increasing temperature. On the other hand, the EDLCPSs revealed this comportment after 240 °C. The rise in thermal PL intensity was assigned to the variation in energy band gap transition and exchanges of the $N_1$ and $N_2$ deep levels nature.

**Keywords** UV light shielding · DGEBA epoxy · 5CB liquid crystal · Optical properties · Vibrational characterization

✉ A. Bouzidi
abdelfattehbouzidi@yahoo.com

[1] Department of Physics, Faculty of Science Sciences and Arts Dhahran Al Janoub, King Khalid University, P.O. Box: 960, Abha 61421, Kingdom of Saudi Arabia

[2] Laboratory of Materials for Energy and Environment, and Modeling (LMEEM), Faculty of Sciences of Sfax, University of Sfax, B.P. 1171, 3038 Sfax, Tunisia

[3] Laboratory of Applied Physics, Faculty of Science, University of Sfax, 3038 Sfax, Tunisia

## 1 Introduction

Several new Liquid Crystals (LCs) and polymer product distributions have recently been developed. An important factor in determining optoelectrical properties is the original feature of LCs used in the Polymer distributed liquid crystals (PDLC). LCs are widely used in display technologies. Due to their fast response time and high transmission and low viscoelastic content, several kinds of research claimed that LCs including fluorine groups are a suitable material for liquid crystal displays (Schadt 2015; Chen et al. 2014; Peng et al. 2016). The PDLCs have been widely studied for flat panels, for example, as candidates for smart windows and holographic films (Liu and Sun 2008; Nicoletta et al. 2005; Park and Hong 2009). PDLCs have been receiving increasing attention recently, mainly because of their suitable potential devices in notebook computers and mobile phones. PDLCs are heterogeneous composite materials composed of micro-droplets of liquid crystal material dispersed in a polymer matrix system (Bronnikov et al. 2013; Sun et al. 2017; Chang and Chen 2013). PDLC represents a new class of optical materials in recent years (Silva et al. 2015; Huang et al. 2013; Kim et al. 2016; Kumar et al. 2011; Trushkevych et al. 2015; Liu et al. 2015) due to their important application in optical devices. The electro-optical properties of the optical system are described in two groups. One of them relates to electro-optical characteristics such as light intensity, transmittance, reflection, efficiency, etc. The photorefractive effect is a phenomenon in which the refractive index of a material is changed by exposure to light. In PDLC, the photorefractive effect is caused by the migration of photo-induced charges in the liquid crystal. When light is incident on a PDLC, the photo-induced charges create a space charge field. This space charge field then changes the refractive index of the liquid crystal, creating a holographic grating (Simoni et al. 1999). He found that when the photorefractive effect occurs, the features of these permanent gratings are explained as a thermal fixation of the changed interfaces. The local heating is used to enhance the photorefractive effect. When a region of the PDLC is heated, the mobility of the photo-induced charges is increased. This allows the space charge field to be created more quickly and efficiently, resulting in a stronger holographic grating. The researchers (Simoni et al. 1999) found that they were able to produce holographic permanent gratings in dye-doped PDLC without the application of external dc voltage by using a combination of the photorefractive effect and local heating. The gratings that they produced were stable and had a high diffraction efficiency. This research is important because it opens the possibility of using PDLC for holographic applications without the need for external dc voltage. This could make PDLC more attractive for use in a variety of applications, such as optical data storage and optical communications. H. Murai et al. analyzed the optoelectrical attributes of thermally cured PDLC film and found that driving voltages could be reduced by adding an excess of hardener in the epoxy resin (Murai and Gotoh 1993). The influence of epoxy monomers including flexible chain segments on the optoelectronic characteristics of thermal-cured PDLC films is studied by Meng et al. (2010). The number of flexible segments in a transistor affects the driving voltages and ON-state transmittance. A transistor with more flexible segments will require lower driving voltages to turn on and will have a higher ON-state transmittance. This is because the flexible segments allow the transistor to be more easily modulated by the gate voltage. When the gate voltage is applied, it creates an electric field that attracts the electrons in the semiconductor material. The more flexible segments there are, the more easily the electric field can be distributed, and the lower the driving voltage required. The ON-state transmittance is the ratio of the current flowing through the transistor to the current that

would flow if the transistor were fully turned on. A transistor with a higher ON-state transmittance will allow more current to flow through it, which is important for applications where high power or high efficiency is required. In general, increasing the number of flexible segments in a transistor will improve its performance. However, there are also some drawbacks to consider. For example, a transistor with more flexible segments will be more complex to fabricate, and it may also be less reliable. This is because the flexible segments act as a buffer between the gate and the channel, reducing the amount of voltage required to turn on the transistor. The increased ON-state transmittance means that more current can flow through the transistor, which can improve the performance of the device. The flexure effect is a promising technology for improving the performance of transistors. It is being used in a variety of applications, including power electronics, radio frequency (RF) devices, and sensors. T. Zhang et al. studied the influence of the functionality of epoxy monomers on the optoelectronic characteristics of thermally cured PDLC films (Zhang et al. 2012). The epoxy monomer is responsible for the crosslinking of the polymer chains in the PDLC film. This crosslinking provides the film with its mechanical strength and helps to prevent it from deforming or breaking. The epoxy monomer also affects the optical properties of the film, such as its refractive index and transparency.

The performance of the epoxy monomer has an important impact on the optoelectro nic and peel strength of thermally cured PDLC films. S. A. Carter et al. studied the morphology of PDLCs and their dependence on the UV polymerization process (Carter et al. 1997). The morphology of the PDLC films can be controlled by adjusting the solidification rate of the polymer matrix and the viscosity of the matrix. By optimizing these factors, it is possible to produce PDLC films with the desired optical properties. They have established that the morphology for the PDLC with an 80% LC fraction mainly is that of the solidification rate of the polymer matrix and the viscosity of that matrix when the separation of the phase is initiated. PDLC films with an 80% LC fraction are often used in smart windows and displays. The optical properties of these films can be changed by applying an electric field, which causes the LC droplets to align or reorient. This can be used to control the amount of light that passes through the film.

In the present work, we aimed to study and characterize the morphological, vibrational, and optical properties of neat epoxy and EDLCP systems. Scanning Electron Microscope (SEM) was studied. Fourier transform infrared (FTIR) and Raman spectroscopy are widely used to obtain information on vibrational properties. The formed systems are examined by UV–visible spectroscopy and photoluminescence.

## 2 Production process

### 2.1 Products and polymer preparation

The epoxy resin is a thermosetting organic polymer called Diglycidyl ether of bisphenol A (DGEBA), which is a compound of bisphenol A and epichlorohydrin. The hardener, Diamino diphenyl sulphone 44DDS, is a diamine that reacts with the epoxide groups in the epoxy resin to form a cross-linked network. The 4′-Pentyl-4-biphenylcarbonitrile 5CB is a small molecule that is added to the mixture to improve the properties of the cured resin. Sigma-Aldrich is a leading supplier of chemicals and laboratory supplies. The chemical structures of the epoxy resin, hardener, and 5CB are shown in Fig. 1. The neat epoxy polymer was prepared by following these steps: (i) The DDS hardener was dissolved in acetone,

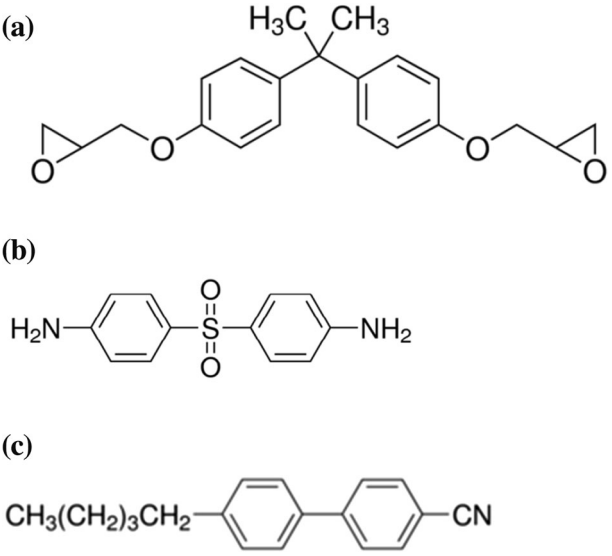


**Fig. 1** Structures of chemical products of (**a**) resin (DGEBA), (**b**) hardener (DDS) and (**c**) liquid crystal (5CB)

ii) The DGEBA resin was added to the DDS solution with a molar ratio of 1:4, (iii) The mixture was deposited on a mold and degassed under vacuum for 2 h at 56 °C. This step is to remove any air bubbles that may be present in the mixture, and (iv) The polymer was then cured under vacuum at 393 K (120 °C) for 21 h. This step is to allow the epoxy resin and hardener to react and form a cross-linked network. Removed disc-shaped of neat epoxy (0.0 wt% 5CB) and EDLCP (5.0 wt% 5CB into DGEBA matrix) samples from the mold have a diameter of 2 cm and a thickness of about 1 mm. Once the samples are obtained, they can be characterized using a variety of techniques.

## 2.2 Techniques

Scanning electron microscopy (SEM) is a technique that uses a beam of electrons to image the surface of a sample. The accelerating voltage of the electron beam in SEM can be adjusted, and a voltage of 20 kV is a typical value for imaging the morphological properties of samples. This is because a lower accelerating voltage will cause less damage to the sample, while still providing sufficient resolution to image the surface features.

The ultraviolet–visible (UV–Vis) spectrometer in the wavelength range of 200–1000 nm is a tool that measures the absorption and transmittance of light by an experiment. The Lambda 950 PerkinElmer is a high-performance UV–Vis spectrometer that is used for an extensive variety of applications, entering the study of optical properties.

Vibrational characteristics of the neat Epoxy and EDLCP systems were likely investigated using a PerkinElmer FTIR spectrometer to determine the frequencies and intensities of the vibrational bands. The vibrational bands are a fingerprint of the material, and they can be used to identify the different types of molecules present in the sample, as well as their concentrations. The KBr matrix is used in FTIR spectroscopy to improve the transmission of the infrared radiation through the sample. KBr is a highly transparent material in the infrared region, and it does not have any strong absorption bands. This makes it a good choice for studying the vibrational properties of other materials. The range of 400–4000 $cm^{-1}$ is a commonly used range for studying the vibrational properties of

materials. This range includes the mid-infrared region, which is important for studying the stretching and bending vibrations of molecules.

The Lab RAM HR (Jobin–Yvon Horiba 800) is a Raman spectrometer that is used to study the vibrational properties of materials. It has a spectral range of 50–4000 $cm^{-1}$, which is a wide range that can be used to study a variety of materials. The He–Ne laser is a common laser that is used in Raman spectroscopy. It has a wavelength of 633 nm, which corresponds to an energy of 1.96 eV. This energy is well-matched to the vibrational modes of many materials, making it a good choice for Raman spectroscopy.

Photoluminescence (PL) spectroscopy is a technique that is used to study the emission of light from a material when it is excited by light. The IHR 320 fluorescence spectrophotometer is a device that is used to measure PL spectra. In the study you mentioned, the photoluminescence spectra of the samples were likely measured at various temperatures to determine the emission wavelengths of the fabricated samples.

## 3 Results and discussion

### 3.1 SEM image characterizations

SEM image is one of the most popular methods used for the characterization of the polymer that provides the investigator with a highly magnified image of the surface of the polymer material.

Figure 2a, b appears the SEM image of both neat epoxy and EDLCPSs, respectively. As presented in this Figure, the neat epoxy sample displays a smooth and clear surface (see Fig. 2a). A similar result agrees with the report by Bouzidi et al. (2018a). Figure 2b revealed that the LC droplets are more evenly sprinkled in the epoxy polymeric matrix. The calculated diameter of the LC droplets is about 0.224 µm. The small LC droplets size (0.224 µm) is also consistent with the presence of nitrile groups. Nitrile groups are known to be surface active, and they can help to stabilize the small LC droplets. As a result, agrees with the report by Z. Jiang et al. (Jiang et al. 2019). It found that the smallest diameter of the LC droplets is small than one µm.

### 3.2 Fourier transform infrared (FTIR) characterization.

FTIR spectra are used to identify the functional groups and the effect of the addition of liquid crystal into a neat epoxy polymer. Figure 3 presents FTIR spectra of neat epoxy polymer and EDLCP. The C-N absorption peak in the 1200–1350 $cm^{-1}$ region is characteristic of the amide linkage, which is present in the polymer (for Both polymer samples). The sulfone stretching vibrations at 1146 and 1360 $cm^{-1}$ are also characteristic of the polymer. The N–H stretching band in the 3400–3500 $cm^{-1}$ regions is also consistent with the presence of amide linkages. The weakness of the oxirane ring characteristic bands ($\nu_{CO}$ at 915 $cm^{-1}$ and $\nu_{CH}$ at 3057 $cm^{-1}$) indicates that the oxirane rings have been opened and the polymerization process is complete. In addition to the spectroscopic evidence, we can also check the physical properties of the samples to confirm that the polymerization process is complete. The peak at 2229 $cm^{-1}$ in the spectrum of EDLCP is attributed to the C≡N stretching vibrational band. This band is characteristic of the nitrile group, which is present

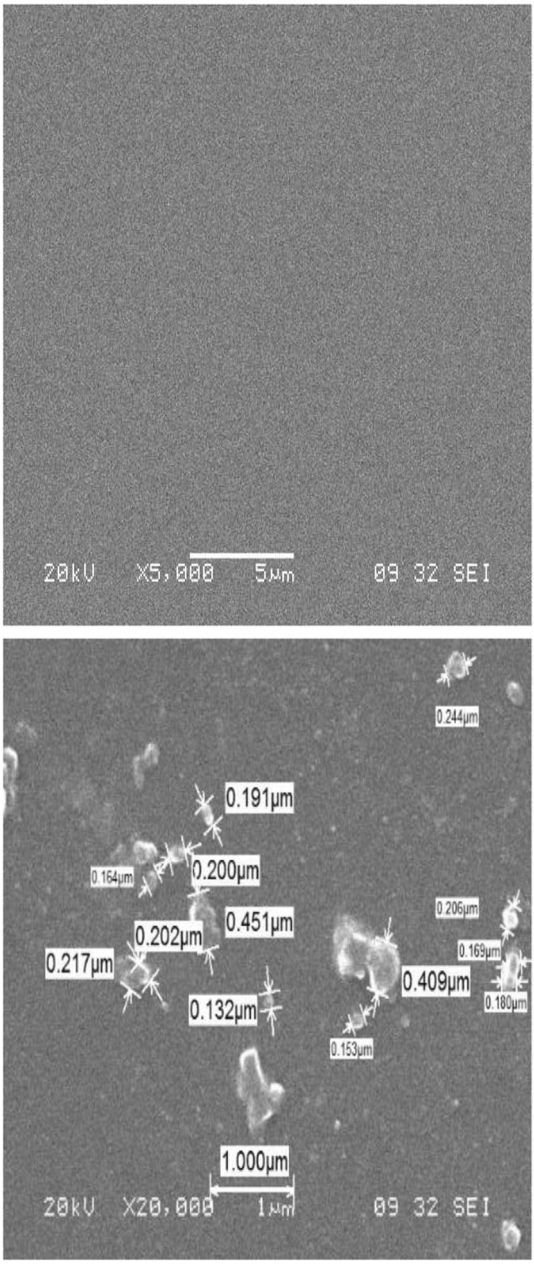


**Fig. 2** SEM image micrograph of both polymeric systems

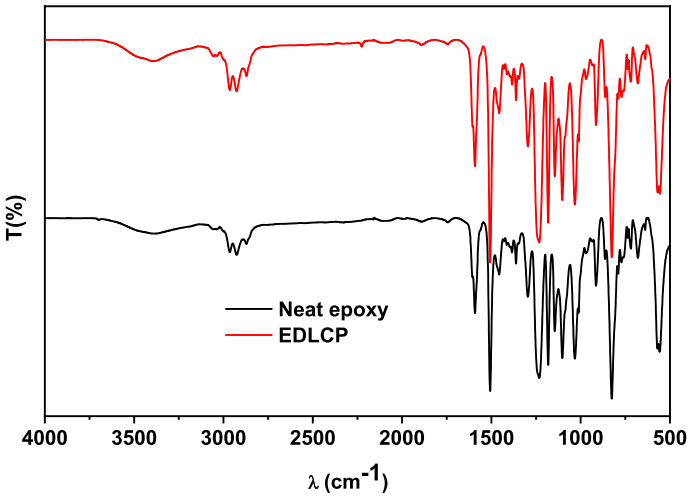


**Fig. 3** FTIR spectra of neat epoxy and EDLCP

in the polymer sample. The nitrile group is formed when the oxirane ring of the polymer sample opens and the amine and carboxylic acid groups react to form an amide linkage.

### 3.3 Raman analysis spectroscopy

Raman analysis spectroscopy is a valuable tool that can be used to confirm the origin of the changes observed via FTIR examination. It is a non-destructive, sensitive, and versatile technique that can be used to identify a variety of molecules. Figure 4 shows the Raman spectra of neat epoxy and EDLCP samples. The deformation band of the epoxy ring and the stretching mode of vibration appear at 640 $cm^{-1}$ and 1225 $cm^{-1}$, respectively. Asymmetrical and asymmetrical vibration of aromatic and methyl (C-H) groups is applied to the overlap observed in the 2875–3076 $cm^{-1}$ range from the FTIR study. In the case of the

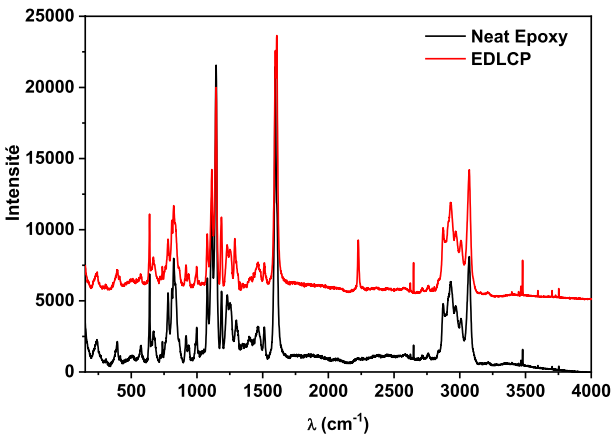


**Fig. 4** Raman spectra of neat epoxy and EDLCP systems

EDLCP sample, we observe the same peaks for the neat epoxy. Meanwhile, we notice the appearance of a new peak in 2229 $cm^{-1}$ attributed to the C≡N stretching vibrational band. These results agree with the FTIR spectra analysis. The agreement between the Raman spectroscopy results and the FTIR spectra analysis suggests that the changes that have been observed are due to the same molecular vibrations. This is further supported by the fact that both techniques are non-destructive and do not damage the sample.

The vibration band at 2229 $cm^{-1}$ in the FTIR and Raman spectra of the EDLCPSs is attributed to the C≡N stretching vibrational band. This is because the C≡N stretching frequency is typically in the range of 2100–2200 $cm^{-1}$. The presence of this band confirms the presence of nitrile groups in the EDLCPSs. Overall, the presence of the C≡N stretching band in the FTIR and Raman spectra of the EDLCPSs is a strong indication that the EDLCPSs contain nitrile groups.

The vibration band at 2229 $cm^{-1}$ in the FTIR and Raman spectra of the EDLCPSs is attributed to the C≡N stretching vibrational band. The C≡N bond is a triple bond, which is made up of a sigma bond and two pi bonds. The sigma bond is the strongest bond between the carbon and nitrogen atoms, and it is responsible for the stretching vibration at 2229 $cm^{-1}$. The pi bonds are weaker bonds, and they do not contribute to the stretching vibration.

The C≡N stretching vibration is a characteristic vibration of nitrile groups. Nitrile groups are found in a variety of molecules, including polymers, dyes, and pharmaceuticals. The presence of the C≡N stretching vibration in the FTIR and Raman spectra of the EDLCPSs confirms the presence of nitrile groups in these materials.

### 3.4 UV–Visible spectroscopy

To investigate the influence of the incorporation of liquid crystal into epoxy matrix we have studied the optical absorbance and transmittance by using UV–visible spectroscopy. Figure 5a, b shows, respectively, the plots of the optical absorbance and transmittance spectra for both neat epoxy polymer and EDLCP samples. In the UV region, plots of neat epoxy and EDLCP exhibit a sharp fundamental absorption edge and their transmittance is relatively poor. The EDLCP system blocks UV light up to a wavelength of about 380 nm, which is the boundary between the UV and visible light spectrum. This means that the EDLCP system can be used to shield devices from harmful UV radiation (Fu et al. 2015; Zhou et al. 2015). The ability of the EDLCP system to block UV light is since the polymer chains in the material absorb photons with wavelengths shorter than 380 nm. This absorption causes the electrons in the polymer chains to be excited, which prevents them from absorbing photons with longer wavelengths. The efficiency of the EDLCP system in blocking UV light can be improved by increasing the concentration of the dopant in the material. This is because the dopant molecules can also absorb photons with wavelengths shorter than 380 nm. The EDLCP system is a promising material for UV light shielding devices. It has the potential to be used in a variety of applications, such as sunscreens, sunglasses, and car windows. These results indicate that such systems may be used in solar cells and various optoelectronic devices as a window layer, such as flats. The incorporation of liquid crystal into epoxy matrix system leads to decrease in the optical transmittance in the visible and near infrared regions. Meanwhile, in the visible and near infrared regions, the transmittance of EDLCP system becomes constant. The development of EDLCP systems for UV light shielding devices is an active area of research. There is still much that is

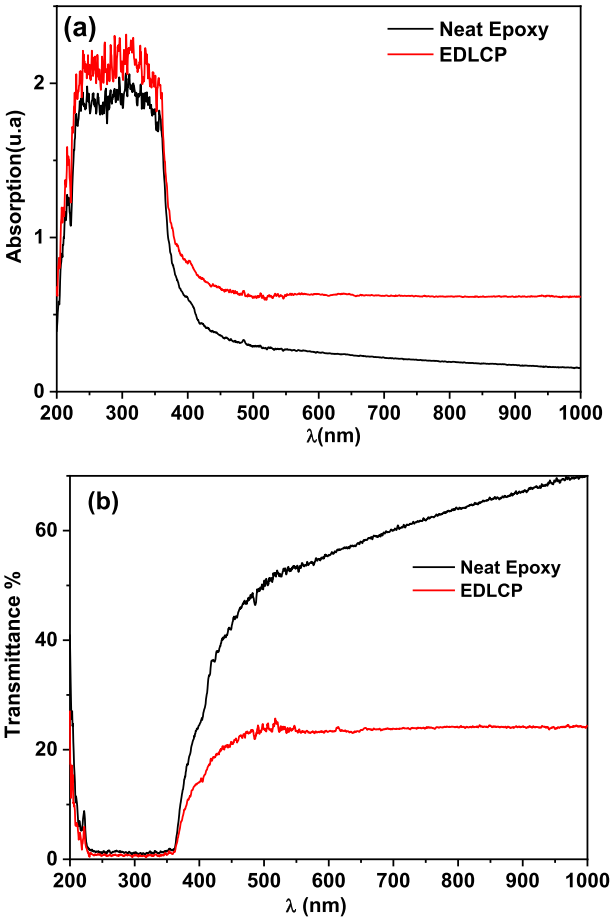


**Fig. 5** UV–vis spectra of neat epoxy polymer and EDLCP: (**a**) absorbance and (**b**) transmittance

unknown about these materials, but the potential benefits of these materials make them a promising candidate for a variety of applications.

The optical band gap was determined using Tauc's relation (Zhou et al. 2015):

$$(\alpha h\upsilon) = B(h\upsilon - E_g)^r \tag{1}$$

where B is a constant depending on a probability of transition, $E_g$ is the band gap energy, hυ is the photon energy incident and r is an exponent characteristic of optical transition which can take the values 1/2 or 2 for allowed direct and indirect transitions respectively.

The energy gap in the optical range has been determined with a plotting $(\alpha h\upsilon)^r$ vs $h\upsilon$ to take intercepts along the linear portion of energy curves of the energy axis of the extensions as shown in Fig. 6a, b. The direct and indirect band gap values are gathered in Table 1. It is clear from Table 1, the direct and indirect band gap values showed a drop with loading of liquid crystal, which related to an increase in the density of defect states. These defects create the localized states in the band gaps. The optical gap is the energy necessary to excite an electron from the valence band to the conduction band. In a disordered material, the atoms are not arranged in a regular lattice, which can lead to localized states in the bandgap. These localized states can trap electrons, making it more difficult for them to be

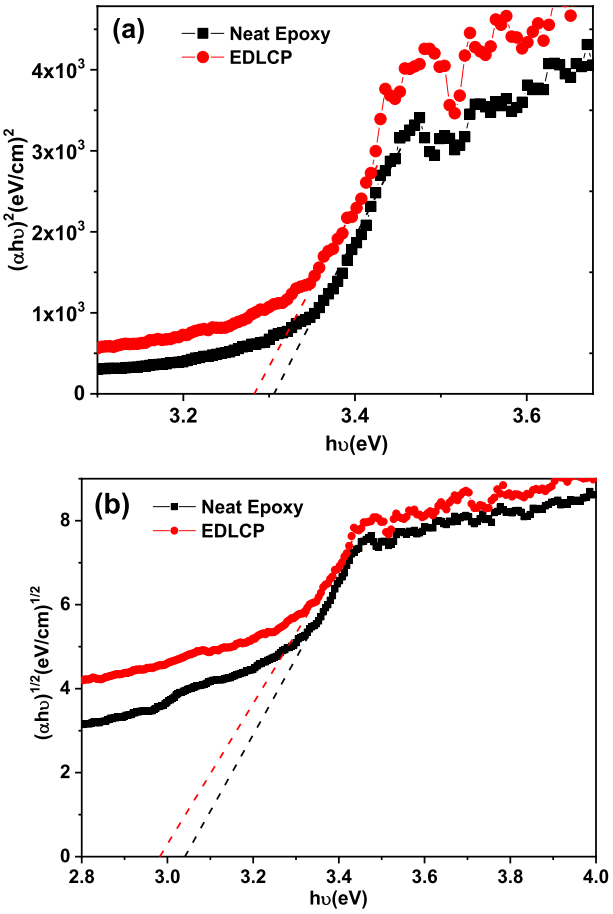


**Fig. 6** Tauc plot for (**a**) direct and (**b**) indirect band gap energy determination of neat epoxy polymer and EDLCP

**Table 1** Calculated values of optical constants

| Samples | Eg(eV) direct | Eg(eV) indirect | $\varepsilon_\infty$ | $\omega_p$(rad/s) | $\tau$(s) | $N/m_e^*$(g$^{-1}$ cm$^{-3}$) |
|---|---|---|---|---|---|---|
| Neat epoxy | 3.30 | 3.04 | 9.11 | $1.37\times10^{14}$ | $1.20\times10^{-11}$ | $4.762\times10^{45}$ |
| EDLCP | 3.28 | 2.98 | 9.18 | $2.36\times10^{13}$ | $5.74\times10^{-13}$ | $1.408\times10^{44}$ |

excited to the conduction band. This results in a decrease in the optical gap. Other authors suggest that the decrease in the optical gap is related to an increase in the degree of disorder in the samples (Moussa et al. 2015; Jilani et al.·2019). This effect has been observed in a variety of disordered materials, including amorphous semiconductors, disordered metals, and glasses. It is also a factor in the optical properties of biological materials. The decrease in the optical gap due to disorder can have a significant impact on the properties of a material. For example, it can affect the material's transparency, conductivity, and photoluminescence. This makes the study of the optical properties of disordered materials an important area of research.

The refractive index ($n$) is an important optical property of polymers. It is a measure of how much light is bent when it passes through the polymer. It is calculated from the following equation (Zhou et al. 2015):

$$n = \frac{1+R}{1-R} + \sqrt{\frac{(1+R)^2}{(1-R)^2} - \left(k^2 - 1\right)} \tag{2}$$

where R is the reflectance and $k = \frac{\lambda\alpha}{4\pi}$ is the extinction coefficient, $\alpha = 2.303A/d$ is the absorption coefficient, A is the absorbance, and d is a parameter represents the thickness of the sample. The variations of the refractive index (n) of both samples over wavelengths are shown in Fig. 7. It is evident from this figure; the refractive index of EDLCP sample is higher than the neat epoxy in the visible and near infrared regions. It found to be 3.03 in this region. The refractive index increases with increasing wavelength and increasing wt% LC which due to the presence of impurities or additives. The highest value of refractive index of EDLCP sample makes this material suitable for optoelectronic devices. The refractive index suggests that the weak response of the EDLC sample is affected by photon energy at long wavelengths in terms of polarization and molecular rotations (Vaghasiya 2016). The addition of liquid crystal (5CB) to an epoxy matrix results in an increase in the refractive index of the material. This is because the refractive index of 5CB is higher than the refractive index of epoxy. The increase in the refractive index is directly proportional to the weight percentage of 5CB in the matrix. The increase in the refractive index is since 5CB droplets in the epoxy matrix scatter the incident light. This scattering causes the light to travel in a more tortuous path, which results in a decrease in the speed of the light. The decrease in the speed of light is what causes the increase in the refractive index. The refractive index of a material is a measure of how much the material bends light. The higher the refractive index, the more the material bends light. The refractive index of a material is also related to the speed of light in the material. The higher the refractive index, the slower the speed of light in the material. The increase in the refractive index of an epoxy matrix with the addition of 5CB can be used to improve the optical properties of the material. For example, the increase in the refractive index can be used to make the material more transparent or to increase its ability to focus light. The increase in the refractive index of an

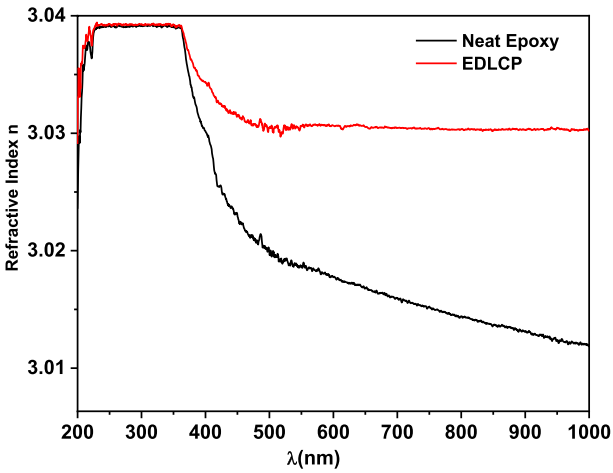


**Fig. 7** The refractive index of the neat epoxy and EDLCP sample

epoxy matrix with the addition of 5CB can also be used to create new optical devices. For example, the material can be used to make lenses, prisms, and waveplates.

The refractive index of a liquid crystal epoxy composite is a complex property that is affected by several factors. However, the understanding of the factors that affect the refractive index can be used to design and optimize liquid crystal epoxy composites for specific applications.

Dielectric properties such as real and imaginary parts for a certain range of wavelength between ultraviolet and near infrared, are significant criteria for the behavior of the investigated materials for various devices. The real part of dielectric permittivity is associated to the dispersion. While the imaginary part is the dissipative rate of electromagnetic wave propagation in the medium. The real ($\varepsilon'$) and the imaginary ($\varepsilon''$) parts of the dielectric permittivity are associated to the refractive index ($n$) and extinction coefficient ($k$) values through the formulas (Ghanipour and Dorranian 2013):

$$\varepsilon' = n^2 - k^2 \tag{3}$$

$$\varepsilon'' = 2nk \tag{4}$$

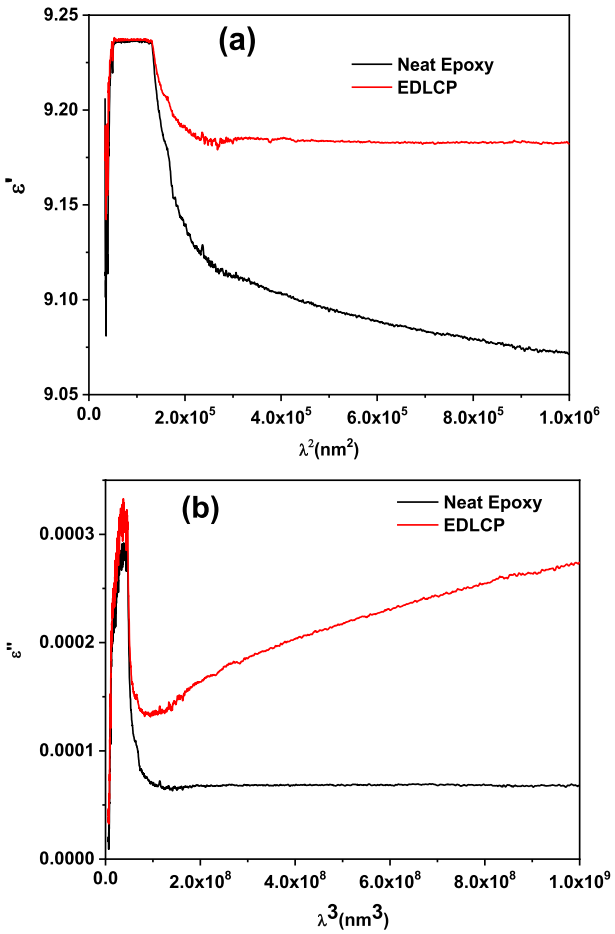


**Fig. 8** Real part of dielectric permittivity versus $\lambda^2$ (**a**) and Imaginary part of dielectric permittivity versus $\lambda^3$ (**b**) for neat epoxy and EDLCP samples

Figure 8a, b shows the dependence on wavelength of (ε′) and (ε″) for neat epoxy and EDLCP samples, respectively. For EDLCP and in the visible-NIR region the real part of dielectric permittivity (ε′) tends to be constant while the imaginary parts of dielectric permittivity (ε″) increases when the wavelength increases. In the visible-NIR region, the real part of the dielectric permittivity of EDLCP samples tends to be constant because the electrons in the material are not excited by the photons in this wavelength range. However, the imaginary part of the dielectric permittivity increases with increasing wavelength because the photons in this wavelength range have more energy and can excite the electrons in the material. This is because the imaginary part of the dielectric permittivity is related to the absorption of light by the material, while the real part of the dielectric permittivity is related to the reflection and refraction of light by the material. In the visible-NIR region, the photons have enough energy to excite the electrons in the material, so they are absorbed by the material. This absorption causes the imaginary part of the dielectric permittivity to increase. The real part of dielectric permittivity for the neat epoxy in the Vis–NIR range decreases when increasing the wavelength and the imaginary parts of dielectric permittivity are found to be constant. The high values of ε′ can be related to the presence of the interfaces within the material. This property makes the samples suitable to be used in high-performance embedded capacitors. In infrared range, the dispersion of ε′ is linear versus the square of the wavelength ($\lambda^2$). While ε″ is linear with ($\lambda^3$) in the same region. This behavior is in good agreement with the classical theory of the dielectric constant, which is expressed by the following relation in the near infrared region ($\omega\tau \gg 1$) (Ghanipour and Dorranian 2013):

$$\varepsilon_1 \approx \varepsilon_\infty - \frac{\varepsilon_\infty \omega_p^2}{4\pi^2 c^2}\lambda^2 \tag{5}$$

$$\varepsilon_2 \approx \frac{\varepsilon_\infty \omega_p^2}{8\pi^3 c^3 \tau}\lambda^3 \tag{6}$$

where $\varepsilon_\infty$ represents the dielectric permittivity at high frequencies, $\omega_p$ is the plasma pulsation, τ is the relaxation time and C is the speed of light in vacuum.

The free carrier concentration with effective mass ratio $N/m_e^*$ is determined as follow (Ghanipour and Dorranian 2013):

$$\omega_p^2 = \frac{4\pi N e^2}{\varepsilon_\infty m_e^*} \tag{7}$$

The obtained values of optical constants are listed in Table 1. As revealed from Table 1, the dielectric permittivity at high frequencies ($\varepsilon_\infty$) of the sample EDLCP is higher than of neat epoxy. This is because the liquid crystal droplets in the epoxy matrix increase the polarizability of the material. Polarizability is a measure of how easily a material can be polarized by an electric field. The higher dielectric permittivity at high frequencies of the EDLCP sample makes it suitable for high-performance embedded capacitor devices. This is because embedded capacitors are used to store electric energy in devices such as smartphones, laptops, and tablets. The higher dielectric permittivity of the EDLCP sample allows it to store more electric energy in a smaller volume, which is an important factor for embedded capacitors. All the other optical parameters are decreased compared to neat epoxy sample.

### 3.5 Photoluminescence

We have studied, for a better investigation of the nature of the excitons and their interaction with the phonons, the temperature dependence of the photoluminescence of the material. The temperature dependence of the photoluminescence of a material can be used to study the nature of the excitons and their interaction with the phonons. The temperature dependence of the photoluminescence spectrum can also be used to study the nature of the excitons. For example, the splitting of the photoluminescence spectrum into two or more peaks can be due to the presence of different types of excitons in the material. Figures 9 and 10 revealed the photoluminescence spectra of neat epoxy and EDLCP samples recorded from 20 to 440 °C with an excitation wavelength of 420 nm. In the temperature range from 20 to 300 °C for the neat epoxy and from 20 to 220 °C for the EDLCP sample, the PL intensity decreased as increasing temperature, which an effect related to the phonon diffusion (i.e., the photo-created pairs electron–hole). At low temperatures, the electron–hole pairs are tightly bound and have a high probability of recombining radiatively, emitting a photon.

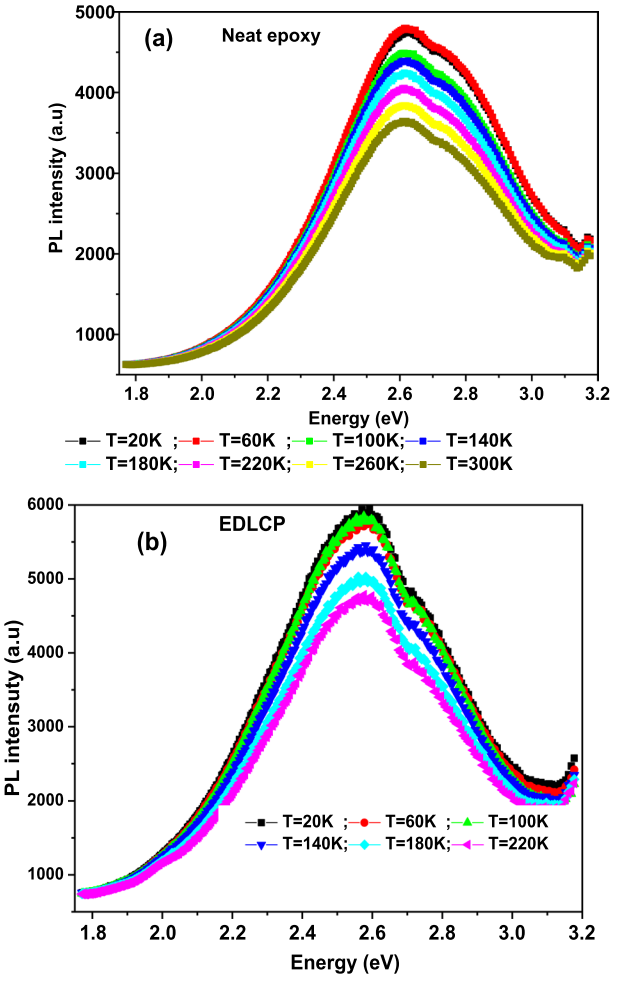


**Fig. 9** The photoluminescence spectra of (**a**) neat epoxy in the temperature range from 20 to 300 °C and (**b**) from 20 to 220 °C for the EDLCP samples

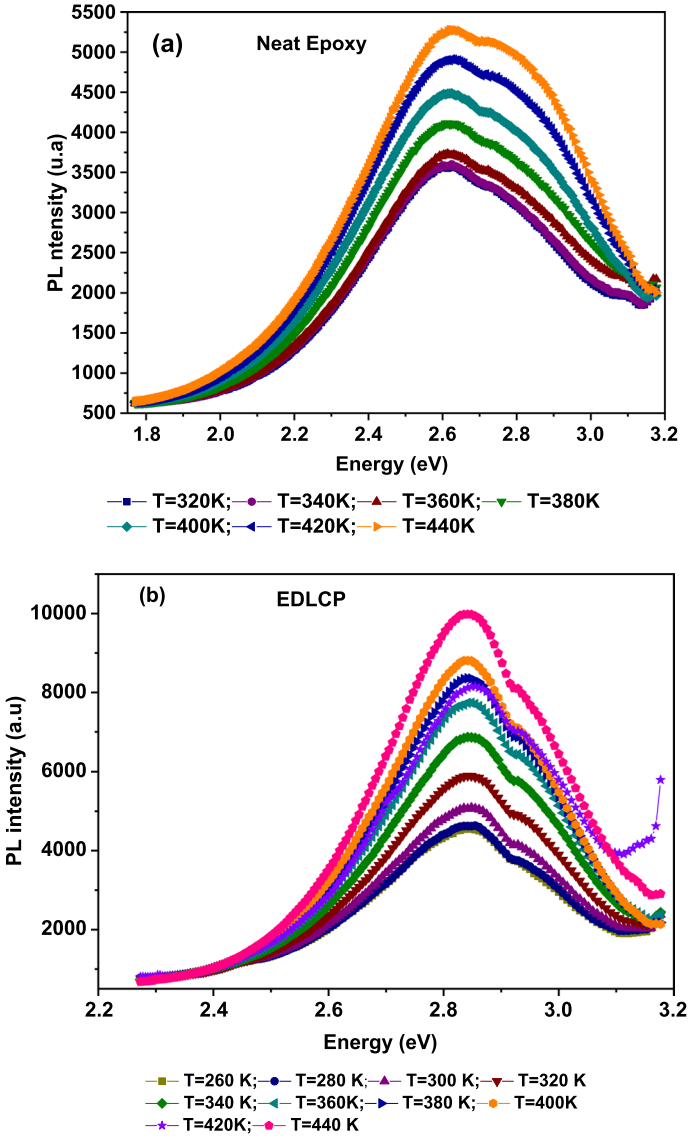


**Fig. 10** The photoluminescence spectra of (**a**) neat epoxy after 300 °C and (**b**) EDLCP sample after 240°C

As the temperature increases, the electron–hole pairs become more loosely bound and have a higher probability of recombining non-radiatively, releasing their energy in the form of heat. This is because the phonons, which are the vibrations of the atoms in the material, can help to break up the electron–hole pairs.

The EDLCP sample has a higher PL intensity than the neat epoxy at low temperatures, but the PL intensity decreases at a faster rate with increasing temperature. This is because the EDLCP sample has more defects and impurities, which act as non-radiative recombination center. The temperature at which the PL intensity starts to decrease is called

the "quenching temperature". The quenching temperature is lower for materials with more defects and impurities. The PL intensity can also be affected by other factors, such as the excitation wavelength, the excitation intensity, and the sample thickness.

After 300 °C, the neat epoxy shows a completely inverted behavior when increasing temperature. However, the EDLCP sample revealed this comportment after 240 °C.

The neat epoxy shows a completely inverted behavior when increasing temperature after 300 °C because the phonon energy becomes high enough to break up the electron–hole pairs even before they can recombine radiatively. This is called "phonon-assisted non-radiative recombination". The EDLCP sample shows this behavior after 240 °C because it has more defects and impurities, which act as non-radiative recombination center. These defects and impurities can trap the electron–hole pairs, preventing them from recombining radiatively (Abdulwahid et al. 2016). The inverted behavior of the PL intensity with increasing temperature is a result of the competition between radiative and non-radiative recombination processes. At low temperatures, the radiative recombination process is dominant, but at high temperatures, the non-radiative recombination process becomes dominant. The inverted behavior of the PL intensity can be used to study the recombination processes in materials. It can also be used to develop materials with improved optical properties.

To investigate the activation energy of neat epoxy and EDLC, we plotted the integrated PL intensity as a function of the temperature inverse (shown in Fig. 11). The temperature dependence of PL integrated intensity cannot be modeled with simple Arrhenius model.

Accordingly, the integrated PL intensity versus the temperature inverse was fitted using the modified Arrhenius model is given by the following equation (Bouzidi et al. 2018b; Ben et al. 2021):

$$I(T) = \frac{I(0)}{\left[1 + a_1 \exp\left(-\frac{E_{a1}}{k_B T}\right)\right]^2} * \left(1 + \frac{A}{\left[1 + \frac{1}{a_2} * \exp\left(\frac{E_{a2}}{k_B T}\right)\right]}\right) \tag{8}$$

where *I(0)* is a proportionality constant, $E_{a1}$ and $E_{a2}$ are thermal activation energies, $a_1$ and $a_2$ are fitting parameters, and $k_B$ is the Boltzmann constant. From the best fits, the values of thermal activation energies are calculated and are grouped in Table 2 for neat epoxy and EDLCP.

A representative scheme was shown in Fig. 12 of PL mechanisms for energy levels $E_{a1}$ and $E_{a2}$ of samples. Where $E_{a1}$ is related to the thermal activation energy needed to extract an electron from the trap level $N_1$ to the Highest Occupied Molecular Orbital (HOMO) level (Kaouach et al. 2013). $E_{a2}$ is attributed to the thermal activation energy needed to extract an electron from the trap level $N_2$ to (HOMO) level.

## 4 Conclusions

This research is focused on the synthesis of neat Epoxy and EDLCP samples and carefully examined their morphological, vibrational, and optical characterization. The morphological properties found that the small size of the LC droplets is about 0.224 µm. The FTIR spectrum peaks correspond to molecular vibrations and chemical interactions, suggesting the presence of a vibration band at 2229 $cm^{-1}$ is attributed to C≡N stretching vibrational band in the EDLCP system. In the UV region, neat epoxy and EDLCP samples block UV

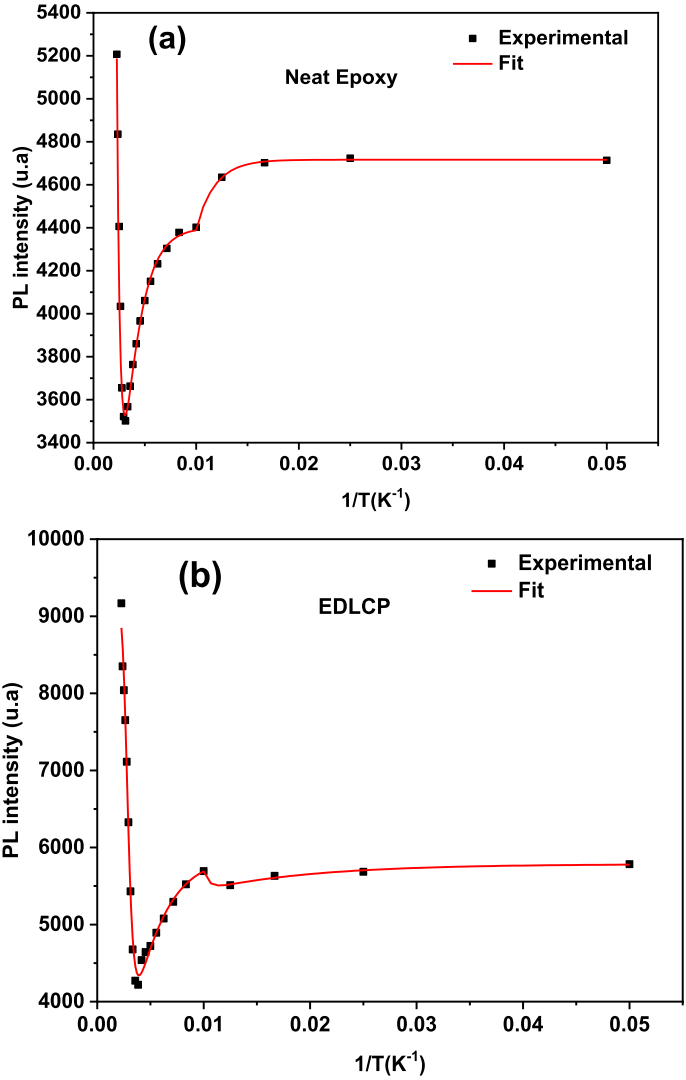


**Fig. 11** The integrated PL intensity as a function of the temperature inverse spectra of (**a**) neat epoxy (**b**) EDLCP samples

**Table 2** The values of thermal activation energies for neat epoxy and EDLCP samples

| Samples | $E_{a1}$ (Mev) | $E_{a2}$ (Mev) |
|---|---|---|
| Neat epoxy | 0.21 | 0.78 |
| EDLCP | 0.32 | 0.90 |

light up to a wavelength of about 380 nm which efficiency of UV light shielding devices. Both the optical band gap decreases with the incorporation of liquid crystal, which contributed to increasing the defect status density. For the photoluminescence (PL) studies and

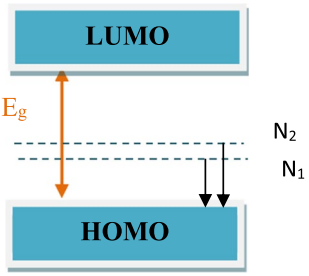


**Fig. 12** Schematic representation of the energy levels $E_{a1}$ and $E_{a2}$

in the temperature range from 20 to 300 °C for the neat epoxy and from 20 to 220 °C for the EDLCP sample, the PL intensity decreased as increasing temperature which an effect related to the phonon diffusion (i.e., the photo-created pairs electron–hole). After 320°C, the neat epoxy shows a completely inverted behavior when increasing temperature. However, the EDLCP sample revealed this comportment after 240 °C. The efficiency of optoelectronic devices is greatly affected by the vibrational properties of the material, which are determined by the interaction of phonons and electron–hole pairs. Understanding PL at different temperatures, EDLCP can make optoelectronic applications more effective.

**Acknowledgements** As part of a small group research project, grant number **RGP1/142/44**, the authors gratefully acknowledge funding provided by the Deanship of Scientific Research at King Khalid University.

**Author contributions** Author contributions: Conceptualization § Methodology: S.E., H.G. and A. B.; Visualization § Data Curation: S.E. and A. B. Analysis § Investigation: H.G. and W. J.; Resources: H. G.; Writing-Original Draft Preparation: A. B. and W.J.; Writing-Review and Editing: A. B., W. J. and H.G.; Validation § Supervision: H. G.; Project Administration: W. J.; Funding Acquisition: H.G, S. E., and W. J.The first draft of the manuscript was written by [A. B.] and all authors commented on previous versions of the manuscript. All authors read and approved the final version of the submitted manuscript.

## Declarations

**Conflict of interest** The authors declare that they have no known competing financial interests or personal relationships that could have appeared to influence the work reported in this paper.

**Data availability** All authors contributed that there is no associated data, or the data will be not deposited. Data sharing is not applicable to this article as no datasets were generated or analyzed during the current study.

## References

Abdulwahid, R.T., Abdullah, O.G., Aziz, S.B., Hussein, S.A., Muhammad, F.F., Yahya, M.Y.: The study of structural and optical properties of PVA:PbO2 based solid polymer nanocomposites. Mater. Sci.: Mater. Electron. 27 (2016) 12112–12118. https://doi.org/10.1007/s10854-016-5363-y

Ben, Y., Liang, F., Zhao, D., Wang, X., Yang, J., Liu, Z., Chen, P.: Anomalous temperature dependence of photoluminescence caused by non-equilibrium distributed carriers in InGaN/(In)GaN multiple quantum wells. Nanomaterials **11**(4) (2021). https://doi.org/10.3390/nano11041023

Bouzidi, A., Omri, K., Jilani, W., Guermazi, H., Yahia, I.S.: Effect of the different concentrations of ZnO: Mn incorporation on the microstructure and dielectric properties of epoxy Nanocomposites. J. Mater. Sci. Mater. Electron. **29**, 5908–5917 (2018a). https://doi.org/10.1007/s10854-018-8563-9

Bouzidi, A., Omri, K., Jilani, W., Guermazi, H., Yahia, I.S.: Incorporation on the microstructure, optical, and dielectric properties of tio2/epoxy composites. J. Inorg. Organomet. Polym. **28**, 1114–1126 (2018b). https://doi.org/10.1007/s10904-017-0772-9

Bronnikov, S., Kostromin, S., Zuev, V.: Polymer-dispersed liquid crystals: progress in preparation, investigation, and application. J. Macromol. Sci., Part B **52**(12), 1718–1735 (2013). https://doi.org/10.1080/00222348.2013.808926

Carter, S.A., LeGrange, J.D., White, W., Boo, J., Wiltzius, P.: Dependence of the morphology of polymer dispersed liquid crystals on the UV polymerization process. J. Appl. Phys. **81**, 5992–5999 (1997). https://doi.org/10.1063/1.364447

Chang, H.L., Chen, C.M.: Polymer matrix on polymer dispersed liquid crystals electro-optical properties. Adv. Mater. Res. **677**, 183–187 (2013). https://doi.org/10.4028/www.scientific.net/amr.677.183

Chen, H., Peng, F., Luo, Z., Xu, D., Wu, S.-T., Li, M.-C., Lee, S.-L., Tsai, W.-C.: High performance liquid crystal displays with a low dielectric constant material. Opt. Mater. Express **4**, 2262–2273 (2014). https://doi.org/10.1364/OME.4.002262

Fu, Y., Huang, Y., Meng, W., Wang, Z., Bando, Y., Golberg, D., Tang, Ch., Zhi, C.: Highly ductile UV-shielding polymer composites with boron nitride nanospheres as fillers. Nanotechnology **26**, 115702 (2015). https://doi.org/10.1088/0957-4484/26/11/115702

Ghanipour, M., Dorranian, D.: Effect of Ag-nanoparticles doped in polyvinyl alcohol on the structural and optical properties of PVA Films. J. Nanomater. **2013**, 1–10. Article ID 897043. https://doi.org/10.1155/2013/897043

Huang, W., Liu, Y., Hu, L., Mu, Q., Peng, Z., Yang, C., Xuan, L.: Second-order distributed feedback polymer laser based on holographic polymer dispersed liquid crystal grating. Org. Electron. **14**, 2299–2305 (2013). https://doi.org/10.1016/j.orgel.2013.05.025

Jiang, Z., Zheng, J., Liu, Y., Zhu, Q.: Investigation of dielectric properties in polymer dispersed liquid crystal films doped with CuO nanorods. J. Mol. Liq. **295**, 111667 (2019). https://doi.org/10.1016/j.molliq.2019.111667

Jilani, W.,·Fourati, N., Zerrouki, C., Gallot-Lavallee, O., Guermazi, H.: Optical, dielectric properties and energy storage efficiency of ZnO/epoxy nanocomposites. J. Inorg. Organomet. Polym. Mater. **29**, 456–464 (2019). https://doi.org/10.1007/s10904-018-1016-3

Kaouach, H., Hosni, F., Daoudi, M., Bardaoui, A., Farah, K., Hamzaoui, H., Chtourou, R.: Effects of gamma irradiation on photoluminescence and activation energy of epoxy resin. Superlattices Microstruct. **55**, 191–197 (2013). https://doi.org/10.1016/j.spmi.2012.10.015

Kim, M., Park, K., Seok, S., Ok, J., Jung, H., Choe, J., Kim, D.: Fabrication of microcapsules for dye-doped polymer dispersed liquid crystal-based smart windows. ACS Appl. Mater. Interfaces **8**, 28241 (2016). https://doi.org/10.1021/acsami.6b12196

Kumar, P., Kang, S., Lee, S., Raina, K.: Analysis of dichroic dye doped polymer-dispersed liquid crystal materials for display devices. Thin Solid Films **520**, 457–463 (2011). https://doi.org/10.1016/j.tsf.2011.06.038

Liu, Y.J., Sun, X.W.: Holographic polymer-dispersed liquid crystals: materials, formation, and applications. Adv. OptoElectron. **2008**, 1–52 (2008). Article ID 684349. https://doi.org/10.1155/2008/684349

Liu, J., Gao, W., Kityk, I.V., Liu, X., Zhen, Z.: Optimization of polycyclic electron-donors based on julolidinyl structure in push–pull chromophores for second order NLO effects. Dyes Pigments **122**, 74–84 (2015). https://doi.org/10.1016/j.dyepig.2015.06.007

Meng, Q., Cao, H., Kashima, M., Liu, H., Yang, H.: Effects of the structures of epoxy monomers on the electro-optical properties of heat-cured polymer-dispersed liquid crystal films. Liq. Cryst. **37**(2), 189–193 (2010). https://doi.org/10.1080/02678290903461402

Moussa, S., Namouchi, F., Guermazi, H.: Elaboration, structural and optical investigations of ZnO/epoxy nanocomposites. Eur. Phys. J. Plus **130**(7) (2015). https://doi.org/10.1140/EPJP/I2015-15152-Y

Murai, H., Gotoh, T.: Stabilization of epoxy-based polymer-dispersed liquid crystal films by addition of excess hardener. Mol. Cryst. Liq. Cryst. Sci. Technol., Sect. A **226**, 13 (1993)

Nicoletta, F.P., Chidichimo, G., Cupelli, D., Filpo, G.D., Benedittis, M.D., Gabriele, B., Salerno, G., Fazio, A.: Electrochromic polymer-dispersed liquid-crystal film: a new bifunctional device. Adv. Funct. Mater. **15**(6), 995–999 (2005). https://doi.org/10.1002/adfm.200400403

Park, S., Hong, J.W.: Polymer dispersed liquid crystal film for variable-transparency glazing. Thin Solid Films **517**, 3183–3186 (2009). https://doi.org/10.1016/j.tsf.2008.11.115

Peng, F., Huang, Y., Gou, F., Hu, M., Li, J., An, Z., Wu, S.-T.: High performance liquid crystals for vehicle displays. Opt. Mater. Express **6**, 717–726 (2016). https://doi.org/10.1364/OME.6.000717

Schadt, M.: Nematic liquid crystals and twisted-nematic LCDs. Liq. Cryst. **42**, 646–652 (2015). https://doi.org/10.1080/02678292.2015.1021597

Silva, M., Sotomayor, J., Figueirinhas, J.: Effect of an additive on the permanent memory effect of polymer dispersed liquid crystal films. J. Chem. Technol. Biotechnol. **90**, 1565–1569 (2015). https://doi.org/10.1002/jctb.4677

Simoni, F., Cipparrone, G., Mazzulla, A., Pagliusi, P.: Polymer dispersed liquid crystals: effects of photorefractivity and local heating on holographic recording. Chem. Phys. **245**, 429–436 (1999). https://doi.org/10.1016/S0301-0104(99)00101-9

Sun, Y., Zhang, C., Zhou, L., Fang, H., Huang, J., Ma, H., Zhang, Y., Yang, J., Zhang, L.-Y., Song, P., Gao, Y., Xiao, J., Li, F., Li, K.: Effect of a polymercaptan material on the electro-optical properties of polymer-dispersed liquid crystal films. Molecules **22**, 43 (2017). https://doi.org/10.3390/molecules22010043

Trushkevych, O., Eriksson, T., Ramadas, S., Edwards, R.: Ultrasound sensing using the acousto-optic effect in polymer dispersed liquid crystals. Appl. Phys. Lett. **107**, 054102 (2015). https://doi.org/10.1063/1.4928390

Vaghasiya, T.K.: The study of change in optical properties of highly AgNO3 doped poly vinyl alcohol hydrosol. Nano Hybrids Compos. **12**, 57–66 (2016). https://doi.org/10.4028/www.scientific.net/NHC.12.57

Zhang, T., Kashima, M., Zhang, M., Liu, F., Song, P., Zhao, X., Zhang, C., Cao, H., Yang, H.: Effects of the functionality of epoxy monomer on the electro-optical properties of thermally-cured polymer dispersed liquid crystal films. RSC Adv. **2**, 2144–2148 (2012). https://doi.org/10.1039/C1RA00562F

Zhou, S., Xu, Q., Xiao, J., Zhong, W., Yu, N., Kirk, S.R., Shu, T., Yin, D.: Consideration of roles of commercial TiO2 pigments in aromatic polyurethane coating via the photodegradation of dimethyl toluene-2,4-dicarbamate in non-aqueous solution. Res. Chem. Intermed. **41**(10), 7785–7797 (2015). https://doi.org/10.1007/s11164-014-1859-3